Journal of Fluorescence, Vol. 15, No. 4, July 2005 (© 2005)
DOI: 10.1007/s10895-005-2825-7

Photochemical Characterization of Up-Converting Inorganic Lanthanide Phosphors as Potential Labels

Tero Soukka,[1,2] Katri Kuningas,[1] Terhi Rantanen,[1] Ville Haaslahti,[1] and Timo Lövgren[1]

Received November 1, 2004; accepted March 17, 2005

We have characterized commercially available up-converting inorganic lanthanide phosphors for their rare earth composition and photoluminescence properties under infrared laser diode excitation. These up-converting phosphors, in contrast to proprietary materials reported earlier, are readily available to be utilized as particulate reporters in various ligand binding assays after grinding to submicron particle size. The laser power density required at 980 nm to generate anti-Stokes photoluminescence from these particulate reporters is significantly lower than required for two-photon excitation. The narrow photoluminescence emission bands at 520–550 nm and at 650–670 nm are at shorter wavelengths and thus totally discriminated from autofluorescence and scattered excitation light even without temporal resolution. Transparent solution of colloidal bead-milled up-converting phosphor nanoparticles provides intense green emission visible to the human eye under illumination by an infrared laser pointer. In this article, we show that the unique photoluminescence properties of the up-converting phosphors and the inexpensive measurement configuration, which is adequate for their sensitive detection, render the up-conversion an attractive alternative to the ultraviolet-excited time-resolved fluorescence of down-converting lanthanide compounds widely employed in biomedical research and diagnostics.

KEY WORDS: Up-conversion; rare earth; autofluorescence; infrared laser diode; immunoassay.

INTRODUCTION

Immunoassays and other ligand binding assays relying on identical principles are widely employed in biomedical research and diagnostic medicine to measure substances of biological interest [1,2]. These substances include various proteins (e.g., antibodies, receptors and enzymes), hormones (thyroxine, steroids and peptide hormones), drugs, and even microorganisms (bacteria and viruses), which can occur in blood and other biological fluids at very low concentrations. The label-based ligand binding methods have established their current position by utilizing the structural specificity characterizing many protein-binding reactions (e.g., the antibody–antigen interaction) and the high-specific activity of non-isotopic labels (e.g., photoluminescent lanthanide chelates and time-resolved fluorometry) enabling extremely low limit of detection and wide applicability. The ideal label technology for these methods is characterized by high signal-to-noise ratio, absence of interfering compounds (in biological samples), good stability (both reagents and signal), rapid and robust signal generation and determination, and low overall cost of the label and detection system [3].

In the immunoassay research there was a considerable pressure during the 1970s to find competitive non-isotopic label substitutes for radioisotopes [4]. Originally, the driving forces in the development were associated with the weak suitability of the radioisotopes for automatic immunoassay analyzers due to the logistic and quality-control problems arising from limited shelf-life of the radiolabeled component, problems of radioactive waste disposal, and the legal constrains due to the fear of health hazards associated with radioactivity [5,6]. In the 1980s the development was promoted further by recognition of the advantages of monoclonal antibodies [7–9]

[1] Department of Biotechnology, University of Turku, Tykistökatu 6A, FIN-20520 Turku, Finland.
[2] To whom correspondence should be addressed. E-mail: tero.soukka@utu.fi

and the crucial importance of the specific activity of the labeled antibody [10,11] in the two-site non-competitive assay design. Although the term specific activity is used in general to indicate the number of observable events, such as emitted photons, yielded per reporter molecule per unit time, the actual detectability of the label depends also on the detection instrumentation and the background signal [12]. One of the most sensitive and versatile label technologies developed, the time-resolved fluorometry of lanthanide chelates with millisecond excited-state lifetime [5,6,13] eliminates the fluorescence background almost completely by utilizing temporal resolution to separate the short-lifetime background and the long-lifetime lanthanide luminescence.

The long-lifetime lanthanide luminescence of certain rare earth complexes is extraordinary in many ways. The lanthanide ions alone are only weakly fluorescent, but when complexed to suitable organic ligands with high absorption coefficient at ultraviolet and suitable triplet-state energy level the luminescence properties become observable [14]. The photoluminescent lanthanide complexes are characterized in that they can be measured with a very wide concentration range (over five orders of magnitude) approaching the dynamic range of luminescence measurement. The very low background fluorescence in time-resolved detection of the lanthanide complexes with millisecond fluorescence lifetime improves also dramatically their limit of detection compared to conventional fluorophores. The lanthanide complexes can be measured either from solution in the same manner than a fluorescent product is measured in the enzyme-label based assays by using dissociation-enhanced lanthanide fluoroimmunoassay principle [15–17] or directly from a solid-phase similar to conventional fluorophores with spatial resolution retained by using intrinsically fluorescent lanthanide chelates and cryptates [18–22]. The emission bands of the lanthanide complexes are very narrow and well separated from the excitation wavelength; the Stokes shift is very large, typically over 250 nm for europium and over 200 nm for terbium complexes. The narrow emission bands enable multiparametric measurements up to quadruple label technology based on europium, terbium, samarium and dysprosium [23,24] and the large Stokes shift contributes to the complete absence of concentration quenching [25], a phenomena commonly observable with conventional fluorescence dyes in high concentration and resulting in a decreasing signal with an increasing labeling degree after only a few labels attached per protein or antibody. The concentration quenching limits also the maximal signal available from polystyrene particles dyed with high concentration of conventional fluorophores—the exact opposite to the ultrabright fluorescence of nanoparticles dyed with tens of thousands of lanthanide complexes [26]. In the homogeneous immunoassays based on fluorescence resonance energy transfer the long-lifetime fluorescence of the lanthanide chelates [27–29] and chelate-dyed nanoparticles [30] has enabled major advantage over conventional fluorophores by eliminating the background originating from the direct fluorescence of the short-lifetime acceptor. In addition, the narrow emission bands are of great benefit as the sensitized emission can be measured at a wavelength of minimal long-lifetime emission of the donor.

An alternative source of long-lifetime lanthanide photoluminescence are inorganic rare earth-based crystals that are commonly used in fluorescent lamps to convert ultraviolet to visible light. Bulk phosphor material (e.g., europium-activated yttriumoxysulphide) can be either ground to submicron particle size [31] or nanocrystals of rare earth oxides, fluorides or phosphates containing europium as a doping element can be synthesized directly [32–34]. The submicron phosphor particles have been stabilized with surface ligands and coated with proteins (e.g., antibodies) and nucleic acids to produce functional conjugates to be employed in ligand binding assays [31], time-resolved fluorescence microscopy [35], and in a homogeneous fluorescence energy transfer assay [36]. These lanthanide phosphors generate photoluminescence typical to the corresponding lanthanide chelates but provide an improved photostability and have slightly different absorption bands for excitation. The lanthanide phosphors designed for mercury discharge lamps have typically excitation bands at a range of the discharge from 254 to 365 nm. The excitation at deep ultraviolet at 254 nm is, however, very weakly suitable for use in fluoroimmunoassays due to the resulting exceedingly high instrument background, which generally has also long decay time. In addition to the excitation bands at ultraviolet, the europium phosphors have been reported to be excited efficiently enough using either violet (390–400 nm) or blue light (465–470 nm) [37], which can moderate the price of the detection system by allowing the use of high-power light emitting diodes as excitation light sources. In the development of photoluminescent lanthanide chelates one of the requirements has been a high excitation wavelength of the ligand, which in practice has been limited to 340–365 nm for europium. Only recently a highly photoluminescent europium complex with excitation maxima over 400 nm has been demonstrated [38]. The ultraviolet-excited time-resolved fluorometry has a noteworthy disadvantage that it requires careful selection of optical components and low-fluorescence coatings in the light-path to avoid long-lifetime background fluorescence and to enable low instrument background.

A new type of particulate reporter, an up-converting phosphor technology introduced in the late 1990s [39,40], provided a novel solution to the problem of instrument background and autofluorescence in the fluorescence-based immunoassays. The up-converting phosphors consist of an inorganic crystal lattice with trivalent rare earth dopands (e.g., yttriumoxysulphide activated with erbium and ytterbium) and they can be fairly similar in structure to the previously described lanthanide phosphors, but possess a unique feature of being capable to convert infrared to visible light via non-coincident absorption of two or three infrared photons [41]. In general, if n photons are involved in the up-conversion process, an n-th order dependence of the photoluminescence emission on excitation power is observed. The efficiency of up-conversion process in these phosphors, however, is greatly enhanced compared to simultaneous two-photon excitation [42], because the trivalent lanthanides commonly have long-lifetime excited states, which can operate as a metastable state excited from a ground state to be excited again to an emission state (or transfer its energy to another ion). This property is so exceptional that no autofluorescence is produced from any biological material at the visible wavelengths by an infrared light flux used to excite the up-converting phosphors; i.e. the anti-Stokes photoluminescence (up-converted emission) can be measured entirely free of autofluorescence and scattered excitation light [39]. In principle, the anti-Stokes photoluminescence background is equivalent to that achieved in luminescence counting, where the dark counts of the photomultiplier set the limit of detection. Further, the up-converting phosphors possess the favorable characteristics associated with lanthanide photoluminescence, including narrow emission bands and large Stokes shift (in this case anti-Stokes shift). The major advantage of the up-converting phosphors as a label in an immunoassay would be the availability of a low limit of detection with an uncomplicated detection system [43]; the anti-Stokes photoluminescence can be measured without temporal resolution using an inexpensive infrared laser diode excitation, standard long-pass color glass as excitation filter, photomultiplier for photon counting and a narrow band-pass filter with adequate infrared blocking for selection of the appropriate emission wavelength.

We describe here an evaluation of anti-Stokes photoluminescence characteristics and chemical compositions of commercially available up-converting inorganic lanthanide phosphors. These phosphors are excited by infrared light at 980 nm and they provide emission from green to red with decay times from tens of microseconds to above a millisecond. The up-converting phosphors characterized here can be ground to submicron particle size to provide a particulate reporter to be coupled with proteins and antibodies. We demonstrate that these reporters provide emission visible by eye without difficulty from transparent solution when illuminated with an infrared laser pointer. Moreover, a fluorescence plate reader is constructed for measurement of anti-Stokes photoluminescence from microtiter wells using an inexpensive infrared laser diode for excitation.

MATERIALS AND METHODS

Phosphor Material

Infrared to visible up-converting anti-Stokes phosphors were acquired from several commercial manufacturers; upconverting phosphor nanopowder (referred later as TAL-IR) was purchased from TAL Materials, Inc. (Ann Arbor, MI), anti-Stokes phosphors FCD-546-1, FCD-546-2, FCD-546-3, FCD-660-2, FCD-660-3 and FCD-660-4 were from Luminophor JSC (Stavropol, Russia), anti-Stokes phosphor LPG-IR-3 was obtained from Platan R&DI (Moscow Region, Russia) and laser detection "anti-Stokes" phosphors PTIR545/UF, PTIR550/F and PTIR660/F were from Phosphor Technology Ltd. (Stevenage, England). In addition, ultraviolet to visible down-converting, narrow-band lamp phosphor FL-612 was obtained from Luminophor JSC. Phosphor compositions and characteristics provided by manufacturers are summarized in Table I.

Elemental Analysis

The up-converting and down-converting phosphors were digested in a microwave digestion unit (Milestone MLS-1200 Mega; Milestone, Sorisole, Italy) with a mixture of 2 ml 96% sulfuric acid and 1 ml 85% orto-phosphoric acid (both of suprapur quality). The phosphor amount in digestion was 50 mg. The digested samples were first diluted to 100 ml and, thereafter, furthermore 100-fold with ion exchanged water. The element compositions of the diluted samples were determined by inductively coupled plasma mass spectrometer (ICP-MS) Perkin–Elmer Elan 6100 DRC Plus (MDS Sciex, Concord, ON). The instrument was calibrated with a commercial standard solution (Spex Multi-Element Plasma Standard ICP-MS-1; MDS Sciex).

X-Ray Powder Diffraction

The structural compositions of the LPG-IR-3 and PTIR545/UF up-converting phosphors were confirmed

Table I. Phosphor Compositions and Physical Properties

Phosphor	Composition	Color	Emission	Diameter (μm)	Density (g/cm^3)
Up-converting phosphors					
TAL-IR	$(Y_{0.86}Yb_{0.11}Er_{0.03})_2O_3$	White	Red	<0.1	—[a]
FCD-546-1	La_2O_2S: Yb^{3+}, Er^{3+}	Pale pink	Green	8–9	6.5
FCD-546-2	Y_2O_2S: Yb^{3+}, Er^{3+}	Pink	Green	8–9	6.0
FCD-546-3	YF_3: Yb^{3+}, Er^{3+}	White	Green	20–25	4.0
FCD-660-2	Y_2O_3 - YOF: Yb^{3+}, Er^{3+}	Pale pink	Red	5–7	5.3
FCD-660-3	YOCl: Yb^{3+}, Er^{3+b}	Pale pink	Red	8–9	5.3
FCD-660-4	YbOCl: Er^{3+b}	Pale pink	Red	8–9	5.7
LPG-IR-3	La_2O_2S: Yb^{3+}, $Er^{3+c,d}$	Pink	Green	4–6	—[a]
PTIR545/UF	Gd_2O_2S: Yb^{3+}, $Er^{3+c,d}$	Pale pink	Green	1.3–2.4[e]	—[a]
PTIR550/F	$NaYF_4$: Yb^{3+}, Er^{3+c}	White	Green	2.3–6.1[e]	—[a]
PTIR660/F	Y_2O_3: Yb^{3+}, Er^{3+c}	Pale pink	Red	2.5–4.8[e]	—[a]
Down-converting phosphor					
FL-612	Y_2O_3: Eu^{3+}	White	Red	3–4	5.0

Note. Data according to manufacturer.
[a] Data not available.
[b] Hydrolytically unstable according to manufacturer.
[c] Rare earth composition based on ICP-MS.
[d] Confirmed by X-ray powder diffraction.
[e] 50% of particle volume.

by an X-ray powder diffraction analysis. The measurements were carried out at room temperature by a Huber 670 image plate (2θ range 4–100°) Guinier camera (Huber Diffraktionstechnik, Rimsting, Germany) using monochromatic copper $K_{\alpha 1}$ radiation ($\lambda = 1.5406$ Å). Data collection time was for 15 min with eight scans of the image plate. Silicon powder (NIST standard 640b) was used as an external standard.

Anti-Stokes Photoluminescence Emission Spectra

Varian Cary Eclipse fluorescence spectrophotometer (Varian Scientific Instruments, Mulgrave, Australia) with standard R928 red-sensitive photomultiplier (Hamamatsu Photonics, Shizuoka, Japan) was equipped with IR laser diode module C2021-F1 (Roithner Lasertechnik, Vienna, Austria) to enable measurement of anti-Stokes photoluminescence emission spectra from a polymethyl methacrylate cuvette (3.5 ml capacity and 10 mm × 10 mm light path) with four clear sides (Kartell, Noviglio, Italy). IR laser diode module and a long-pass filter glass RG-850 (Andover Corporation, Salem, NH) were mounted to a cuvette holder of the spectrophotometer. The laser module was aligned to the excitation light path and the emitted light was collected to an emission monochromator at 90° angle to the laser beam. The laser module was connected to an external power source and the spectra were collected using bio/chemiluminescence mode of the fluorescence spectrophotometer from 350 to 850 nm (without any emission filter, i.e. filter setting open) by 0.75 nm resolution with 2.5 nm emission slit.

Anti-Stokes Photoluminescence Intensity and Decay Spectra

Plate Chameleon instrument obtained from Hidex (Turku, Finland) was modified for measurement of anti-Stokes photoluminescence intensity from the up-converting phosphors by replacing the original excitation light source (Xenon flash lamp) by an IR cw laser diode module C2021-F1 (Roithner Lasertechnik) with optical output power of 200 mW and peak wavelength at 980 nm. The excitation pathway was converted to reflect the focused laser beam to microtiter well using a small-diameter aluminium mirror (Finnish Specialglass, Espoo, Finland). The excitation filter was a long-pass filter glass RG-850 (Andover Corporation). The fluorescence emission was collected to emission filter by two plano-convex lenses (Melles Griot, Irvine, CA) mounted in the emission pathway and focused onto the blue-green sensitive bialkali photocathode of the 9102 KB end-window photomultiplier tube (Electron Tubes, Ruislip, England) by a plano-convex lens and an enhanced aluminium mirror. Band-pass emission filters 535/50 nm (center wavelength = 535 nm, half width = 50 nm, peak transmittance ≥60%; Bk Interferenzoptik Elektronik, Nabburg, Germany), 616/7 nm (peak $T \geq 75\%$; Ferroperm, Vedbaek, Denmark), 660/25 nm (peak $T \geq 70\%$; Bk In-

terferenzoptik Elektronik) and short-pass filter <775 nm ($T \geq 85\%$ from 450 to 675 nm; Andover Corporation), all 25.4 mm in diameter, provided high blocking at laser diode wavelength. If necessary, the photoluminescence emission was attenuated by an absorptive neutral density filter (optical densities 2.0 and 3.0, i.e. average transmittances 1 and 0.1%, respectively; Thorlabs, Newton, NJ) combined with an emission filter. Photoluminescence intensity was measured by exposing phosphor suspension placed in black microtiter well (Greiner Bio-One, Kremsmuenster, Austria) to IR laser beam with an optical power density of $>40\,\mathrm{W\,cm^{-2}}$ for 2000 ms excitation time and counting photoelectrons at the same time. Time-resolved photoluminescence emission decay spectra at 535 nm and at 665 nm were recorded with 20 μs resolution using 3.5 ms excitation time and total recording time of 20 ms. Typically, the decay spectrum was integrated for 1000 cycles of excitation. Thereafter, the decay parameters were obtained by fitting the curve to multiexponential decay using Origin 6.0 (OriginLab, Northampton, NA).

Time-Resolved Fluorescence Emission, Excitation and Decay Spectra

Fluorescence emission, time-resolved fluorescence emission and emission decay spectra of the FL-612 ultraviolet-excited lamp phosphor were measured from phosphor suspension with Varian Cary Eclipse fluorescence spectrophotometer (Varian Scientific Instruments) using a standard cuvette holder. Emission spectra were measured using a polymethyl methacrylate cuvette (3.5 ml capacity and 10 mm × 10 mm light path) with four clear sides (Kartell), and excitation and emission decay spectra were recorded using a synthetic quartz cuvette with similar dimensions (Hellma, Müllheim, Germany). The time-resolved fluorescence emission spectrum was measured using phosphorescence mode of the fluorescence spectrophotometer and excitation wavelength of 265 nm (excitation slit 20 nm and filter 250–395 nm) from 350 to 850 nm (emission slit 2.5 nm and no emission filter) by 0.75 nm resolution using 200 μs delay and 400 μs gate time. Transmission through a clear side of the polymethyl methacrylate cuvette at 265 nm was over 45%. Emission spectrum was measured also in fluorescence mode using equal settings except no temporal resolution. Time-resolved excitation spectrum was measured using phosphorescence mode and emission wavelength of 612 nm (emission slit 10 nm and filter 550–1100 nm) from 230 to 580 nm (excitation slit 2.5 nm and filter setting auto) by 0.75 nm resolution using 150 μs delay and 600 μs gate time. Decay spectrum was recorded at emission wavelength of 612 nm (emission slit 10 nm and filter 550–1100 nm) using excitation wavelength of 265 nm (excitation slit 20 nm and filter 250–395 nm). The data was integrated for 100 cycles of excitation by 20 μs temporal resolution and total decay time of 10 ms.

Time-Resolved Fluorescence Intensity

Photoluminescence intensity of the FL-612 ultraviolet-excited lamp phosphor was measured from suspension samples placed in microtiter wells by Wallac Victor (PerkinElmer Life and Analytical Sciences; Wallac Oy, Turku, Finland) with standard R1527 side-window photomultiplier tube (Hamamatsu Photonics) using time-resolved fluorescence mode. The measurement was performed using europium measurement protocol (delay time 400 μs, window time 400 μs, cycle time 1000 μs; typically counts for 1000 cycles were integrated) with Xenon-flash energy set to maximum value and excitation filter changed to D320 wide-band color glass emission filter (standard filter in the instrument). Emission wavelengths were selected by band-pass filters 616/7 nm (peak $T \geq 75\%$; Ferroperm), 665/7.5 nm (peak $T \geq 75\%$; Barr Associates, Westford, MA) and short-pass filter <775 nm ($T \geq 85\%$ from 450 to 675 nm; Andover Corporation) all 25.4 mm in diameter. If necessary, the photoluminescence emission was attenuated by an absorptive neutral density filter (optical density 2.0; Thorlabs) combined with an emission filter.

Bead-Milling and Purification

The PTIR550/F up-converting phosphor was bead-milled and purified to produce colloidal phosphor particle suspension. Zirconia/Silica beads 0.1, 1.0 and 2.5 mm in diameter (Biospec Products, Bartlesville, OK) (0.95, 0.85 and 1.4 g, respectively), 0.85 g of PTIR550/F phosphor and 2 ml DMSO were added to a 4-ml glass vial (inside diameter 15 mm). The grinding was performed by vigorously shaking the glass vial containing the phosphor and bead suspension in Vortex Genie II (Scientific Industries, Bohemia, NY) for 24 h using power-level 8, and after addition of 0.85 g of Zirconia/Silica beads 0.5 mm in diameter (Biospec Products), continuing the shaking for additional 24 h using power-level 10. The colloidal phosphor particles were purified from the grinding beads by diluting the phosphor slurry into DMSO (12 ml total volume) and allowing the suspension to settle down in a 15-ml test tube for 2 h before repeating the procedure twice for the uppermost 8–10 ml volume containing the colloidal phosphor particles (without any grinding beads). There-

after, the uppermost phosphor suspension was divided into four 2 ml aliquots. Each of the aliquots was washed first by 1.25 ml of mixture of DMSO/H_2O (60:40), then by 1.25 ml of acetone and finally by 1.25 ml of DMSO, using centrifugation (over 8000 g, 20 min) to precipitate the particles and bath sonication (Finnsonic m03; Finnsonic, Lahti, Finland) for resuspension. The washed particles were resuspensed into 1.5 ml of DMSO and stored in slow rotation (Rotamix; Heto Lab Equipment, Allerød, Denmark) at room temperature. The concentration of the colloidal phosphor particles was measured by transferring a known volume of suspension into a pre-weighted filter tube (VectaSpin Micro with Anopore 0.02 μm membrane; Whatman, Brentford, England), washing the particles with ethanol and weighting the dried filter. The size distribution profile of the colloidal phosphor particles was measured in 10 mM borate-buffer, pH 8.5, containing 0.1% Tween 20 using Coulter N4 plus submicron particle size analyzer (Beckman Coulter, Fullerton, CA, USA).

RESULTS AND DISCUSSION

The rare earth compositions and physical properties of the 11 characterized commercial up-converting phosphors and one down-converting phosphor are shown in Table I. The term down-conversion is used here to mean absorption of one higher energy photon and emission of a single lower energy photon, and not quantum cutting which can generate up to two emitted photons from a single absorbed higher energy photon [44]. The phosphors have an average particle size between 1 and 10 μm, except the TAL-IR upconverting phosphor nanopowder, which is the only submicron-sized phosphor with particle size below 0.1 μm, and the FCD-546-3 anti-Stokes phosphor, whose particle size is between 20 and 25 μm. The structural compositions of the phosphors except for two phosphors were obtained from the manufacturers. The structural composition of the LPG-IR-3 and PTIR545/UF up-converting phosphors were analyzed as La_2O_2S and Gd_2O_2S, respectively, by routine X-ray powder diffraction analyses. The composition of the LPG-IR-3 was verified later as $La_2O_2S:Yb^{3+},Er^{3+}$ by the manufacturer. The FCD-660-3 and FCD-660-4 phosphors were reported as hydrolytically unstable. The analysis of element concentrations of the phosphors by ICP-MS allowed verification and comparison of the rare earth compositions of the phosphors. The determined concentrations of Y, La, Gd, Yb, Er and Eu, shown in Table II, were consistent with the reported chemical and structural composition. The TAL-IR was the only phosphor, where the manufacturer reported the element ratios. The manufacturer of the PTIR545/UF, PTIR550/F and PTIR660/F did not disclose the rare earth composition, and the phosphor compositions were specified only as rare earth oxysulphide, sodium rare earth fluoride and rare earth doped yttrium oxide, respectively.

The photoluminescence emission spectra were measured for the up-converting phosphors (Fig. 1A–K) using 980 nm laser excitation and for the down-converting phosphor (Fig. 1L) using a Xenon flash excitation in fluorescence spectrophotometer. The temporal resolution was essential in the measurement of the down-converting phosphor to avoid measurement of the ultraviolet-excited

Table II. Phosphor Element Concentrations

Phosphor	Element concentration[a] (μmol/g)				
	Y	La	Gd	Yb	Er
Up-converting phosphors					
TAL-IR	6165 ± 122	0.1 ± 0.01	0.0 ± 0.01	770 ± 12	201 ± 2.5
FCD-546-1	38.9 ± 0.95	6577 ± 101	0.9 ± 0.02	226 ± 3.5	141 ± 2.1
FCD-546-2	6089 ± 113	5.8 ± 0.1	7.3 ± 0.1	584 ± 16	277 ± 2.1
FCD-546-3	4119 ± 53	0.6 ± 0.01	0.5 ± 0.01	951 ± 17	122 ± 2.0
FCD-660-2	6475 ± 122	0.7 ± 0.01	0.1 ± 0.01	668 ± 15	246 ± 2.4
FCD-660-3	3971 ± 42	1.9 ± 0.1	0.1 ± 0.01	1556 ± 27	71.2 ± 1.2
FCD-660-4	230 ± 1.7	0.1 ± 0.01	1.0 ± 0.02	3265 ± 53	155 ± 1.9
LPG-IR-3	29.8 ± 0.24	6938 ± 146	0.2 ± 0.01	189 ± 2.4	137 ± 1.5
PTIR545/UF	13.0 ± 1.1	0.0 ± 0.01	2262 ± 57	1138 ± 27	285 ± 4.8
PTIR550/F	2767 ± 48	0.5 ± 0.01	0.2 ± 0.01	777 ± 20	79.5 ± 1.4
PTIR660/F	6420 ± 114	0.1 ± 0.01	3.3 ± 0.04	225 ± 2.3	370 ± 5.2
	Y	La	Gd	Yb	Eu
Down-converting phosphor					
FL-612	10865 ± 151.2	0.2 ± 0.03	0.1 ± 0.02	0.2 ± 0.01	678.9 ± 49

[a] Values are given with ± SD.

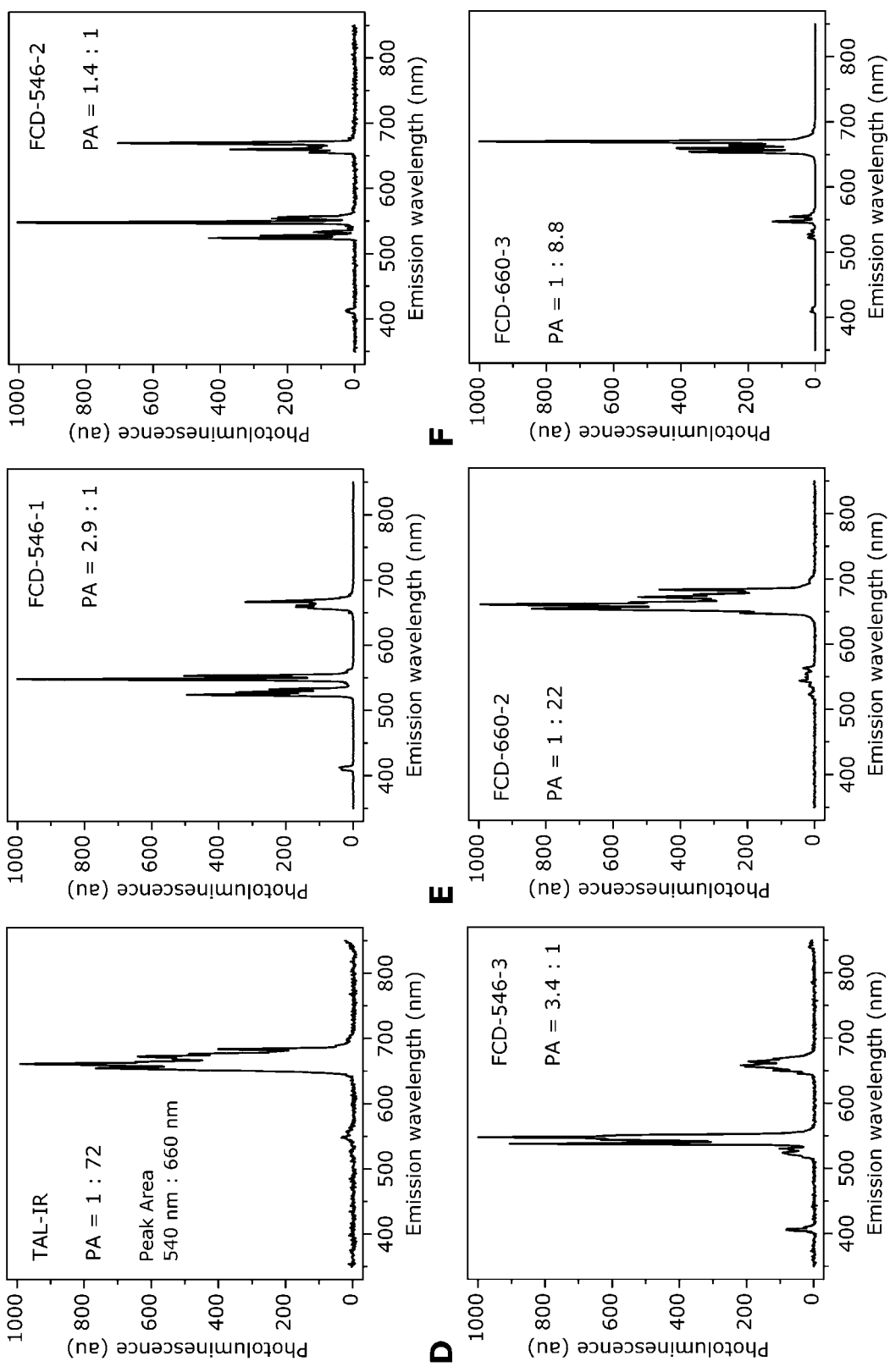

Fig. 1. Emission spectra of different phosphors. IR laser-excited anti-Stokes photoluminescence spectrum of (A) TALIR, (B) FCD-546-1, (C) FCD-546-2, (D) FCD-546-3, (E) FCD-660-2, (F) FCD-660-4, (G) FCD-660-4, (H) LPG-IR-3, (I) PTIR545/UF, (J) PTIR550/F, and (K) PTIR660/F phosphors and (L) ultraviolet-excited fluorescence (*solid line*) and time-resolved fluorescence (*dashed line*) spectrum of FL-612 phosphor. The spectra were measured in DMSO at room temperature. The phosphor concentrations varied from 6.7 μg/ml (LPG-IR-3, FCD-546-2 and FCD-660-4) to 200 μg/ml (TAL-IR and FL-612). *Note.* au, arbitrary unit; PA, ratio of green to red emission peak area was calculated by integrating photoluminescence intensity from 500 to 580 nm (green) and from 620 to 700 nm (red).

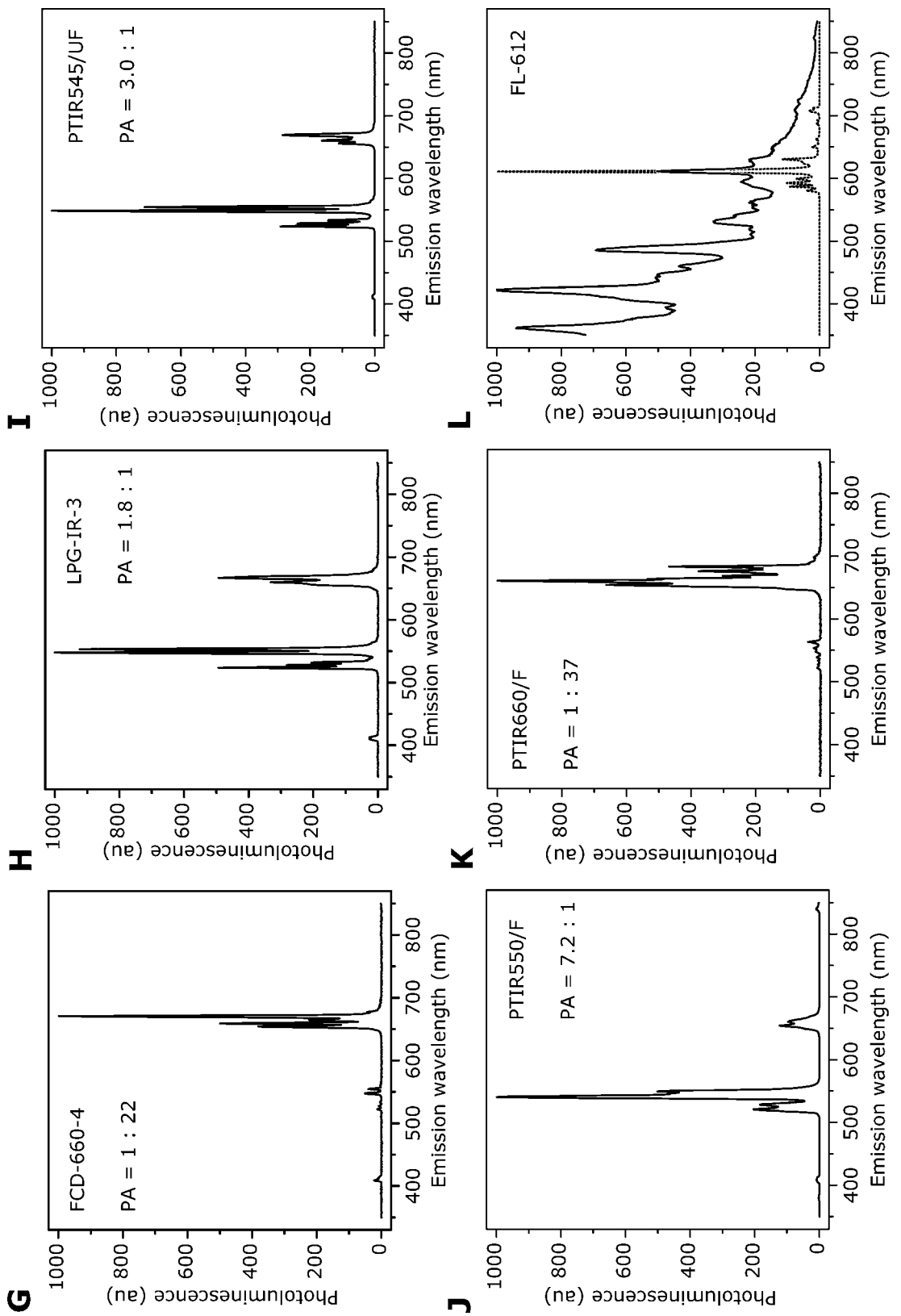

Fig. 1. Continued.

fluorescence originating from the instrument and the cuvette. The excitation wavelength for the down-converting phosphor was shifted to 265 nm because absorption of the cuvette was excessive below 260 nm. The green to red emission ratio of the up-converting phosphors varied from 1:72 to 7.2:1. There was no obvious linkage between Yb^{3+} to Er^{3+} concentration ratio (calculated from Table II) and the green to red emission ratio. The emission ratio was more related to the host material. Because even the TAL-IR phosphor generating the purest red emission had green to red emission ratio below one to hundred, the simultaneous use of the red and green emitting up-converting phosphors for multiplexed detection [40,45] is somewhat limited. The green up-converting phosphors and also some of the red phosphors produce also a third small emission band at 410 nm. It is still possible to realize multiplexing by using phosphors with different rare earth emitter ion to change ion-specific emission properties [40], e.g., Tm^{3+} or Ho^{3+} instead of Er^{3+} would produce blue (475 nm) or green (545 nm) emission, respectively.

The photoluminescence emission intensities of the up-converting phosphors were measured using a fluorescence plate reader equipped with 980 nm laser excitation (Fig. 2). Band-pass filters in the Chameleon instrument were selected for the emission bands at wavelengths 535 and 665 nm, and for an emission minimum at 616 nm, based on the emission spectra. The laser beam was focused through a small-diameter mirror to the microtiter well using a collimator optics integrated into the laser module. The cross-section of the focused laser beam in the microtiter well was approximately $2.4 \times 10^{-3}\,cm^2$ ($300\,\mu m \times 800\,\mu m$) resulting in a power density over $40\,W\,cm^{-2}$, comparable to the power density reported earlier [46]. For the down-converting phosphor, narrow band-pass filters with center wavelengths at 616 and 665 nm were chosen, and the photoluminescence emission intensities were measured using a time-resolved fluorescence plate reader with Xenon flash excitation. In the Victor instrument the 254 nm excitation band of the FL-612 phosphor could not be excited, which limited the total fluorescence signal in the measurement. The cross-section of the focused flash pulse in the microtiter well, however, was larger than $30 \times 10^{-3}\,cm^2$ (1 mm × 3 mm), which means that the measured signal is generated in a volume over tenfold larger than in the Chameleon instrument. In addition to the emission intensities chosen by the band-pass filters, the total photoluminescence intensities within a spectral range of 450–675 nm were measured for

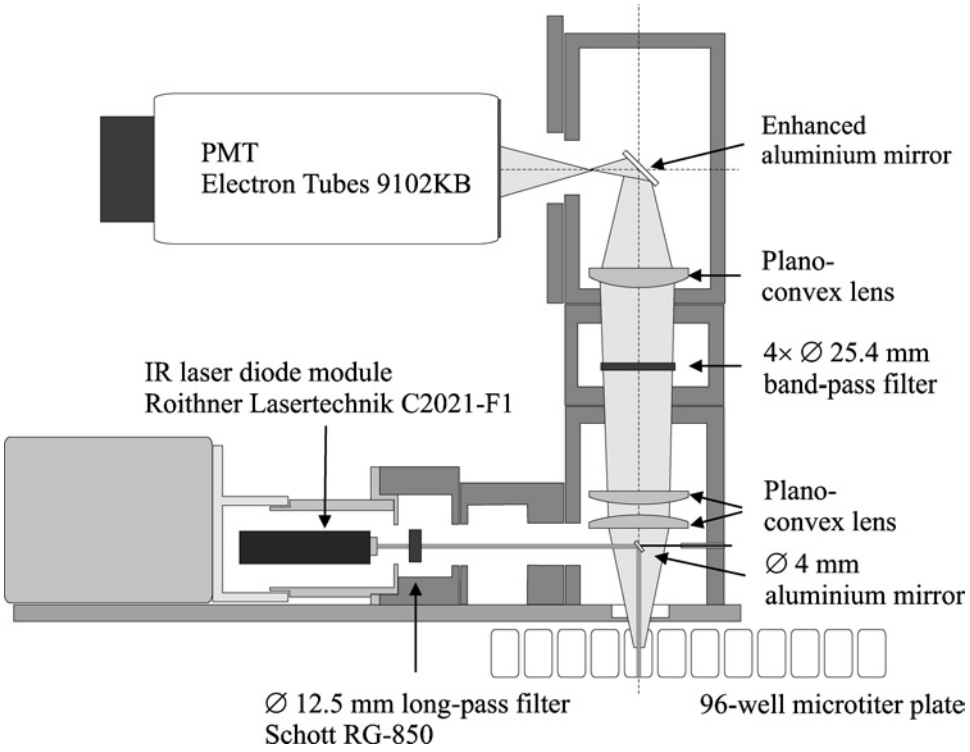

Fig. 2. Diagram of the microtiter plate fluorometer for anti-Stokes photoluminescence. The Plate Chameleon instrument is based on an epifluorescence set-up and includes an xy-conveyor for movement of microtiter plate. *Note*. PMT, photomultiplier tube.

both the up-converting and down-converting phosphors using a 775 nm short pass filter.

The photoluminescence intensities of the up-converting and down-converting phosphors measured with different emission filters are shown in Table III. The phosphor with the highest photoluminescence intensity, LPG-IR-3, is detectable down to pg/ml concentrations, assuming that the signal response is linear to concentration. The photoluminescence intensities between phosphors, however, varied significantly; the up-converting phosphor with the weakest intensity, TAL-IR, was over 10,000-fold weaker than the LPG-IR-3 when the total photoluminescence was compared. The yttriumoxide-based TAL-IR, FCD-660-2 and PTIR660/F up-converting phosphors yielded generally the weakest photoluminescence intensities. There was a weak linkage between Yb^{3+} to Er^{3+} concentration ratio and intensity as well as between dope concentration and intensity; the highest photoluminescence intensity was produced by the smallest excess of Yb^{3+} and by the lowest total dope concentration. It has been reported, that the photoluminescence intensity tends decrease with increasing concentration of Er^{3+}, because high dope concentration will lead to self-quenching due to cross-relaxation processes [47]. The standard deviations of the photoluminescence intensities measured were relatively large due to small excitation cross-section and the tendency of the phosphors to settle down in the microtiter wells. The green to red photoluminescence emission ratios obtained from integrated emission peak areas (Fig. 1) were significantly smaller than the ratios calculable from emission band intensities at green (535 nm) and red (665 nm) shown in Table III. In both cases, however, the most intense bands are the same and agree with the principal emission color reported for the phosphor. The difference between the methods is due to red-sensitivity difference of the photomultipliers in the fluorescence spectrophotometer and the plate reader. The emission ratios calculated from the photoluminescence intensities resemble more the visual appearance of the emission color, because human eye is also more sensitive to green light.

The principles of down-conversion and up-conversion are spectrally illustrated in the Fig. 3. In addition to the major band at 254 nm, the time-resolved fluorescence excitation spectrum of the FL-612 down-converting phosphor contains minor excitation bands at approximately 300, 320, 400, 470 and 530 nm. The distinct feature of the ionic photoluminescence, the narrow emission peaks conventionally associated with the lanthanide chelates and observed with the FL-612 down-converting phosphor, are also a definite feature of the characterized up-converting inorganic lanthanide phosphors. The emission spectra of the PTIR550/F up-converting phosphor and the FL-612 down-converting phosphor (insert in Fig. 3) are compared in log-scale in the Fig. 4. The narrowness of the emission peaks of the up-converting phosphor stands well comparison with the time-resolved fluorescence emission spectra of the europium-based phosphor and also of other lanthanide complexes [30,48]. The difference in photoluminescence intensity in the PTIR550/F up-converting phosphor emission spectrum between the peak at 540 nm and minimum at 600 nm is at least three orders of magnitude. The actual difference is apparently greater, because intensity in the spectrum at 600 nm is at the level of instrument background. This was further supported by the photoluminescence intensity difference between measurements at 535 and 616 nm, which still exceeded four orders of magnitude after the difference in bandwidth and transmission of the filters was taken into consideration. Based on the intensity measurements, the other two up-converting phosphors, FCD-546-1 and LPG-IR-3, have indeed a larger contrast between 535 and 616 nm than the PTIR550/F up-converting phosphor. The photoluminescence intensity difference of FL-612 down-converting phosphor between the peak at 616 nm and a local emission minimum at 665 nm is significantly smaller.

The fluorescence decay times of the up-converting phosphors in DMSO where measured after a laser excitation pulse of 3.5 ms allowing the photoluminescence to stabilize on a steady level during the excitation. The decay spectrum was measured thereafter by 20 μs resolution, which was known to limit the decay time analysis only to decays of tens of microseconds and longer. This was not considered a serious limitation as the lifetimes were expected to be in the range from microseconds to several milliseconds, which are typical to photoluminescence of down-converting lanthanide compounds. This assumption was confirmed as the signal started to decay from the steady level without any immediate drop after the excitation, as shown in Fig. 5A. The decay curves, however, did not fit to a single exponential decay, but were either dual or triple exponential, and the decay times of the individual components varied from 23 to 1490 μs (Table III). The decay times measured from Er^{3+} doped fluoride glasses for the 550 nm anti-Stokes emission excited by three-photon process with 800-nm pumping have been in the same range varying from 15 μs to 3.2 ms [49]. The observed decay times of the red emission $^4F_{9/2} \rightarrow ^4 I_{15/2}$ (665 nm) were regularly longer than those of the green emission $^2H_{11/2}/^4S_{3/2} \rightarrow ^4 I_{15/2}$ (535 nm). This is assumed to relate to population of the $^4F_{9/2}$ level, from where the red emission originates, by relaxation processes from the $^2H_{11/2}$ and $^4S_{3/2}$ levels (Fig. 6) [50]. The longest decay time

Table III. Phosphor Photoluminescence Properties

	Photoluminescence Intensity[a] (cts)			Photoluminescence Decay[b] (μs)		
Phosphor	535/50 nm[c] (ND 3.0)	616/7 nm[c] (–)	665/25 nm (ND 2.0)	<775 nm (ND 3.0)	535/50 nm (τ_1, τ_2 [, τ_3][d])	665/25 nm (τ_1, τ_2 [, τ_3][d])
Up-converting phosphors						
TAL-IR	119 ± 22	1 ± 26	3891 ± 149	1356 ± 58	43, 117	66, 212
FCD-546-1	3027000 ± 1097000	2249 ± 722	2963000 ± 1076000	5097000 ± 1581000	72, 155, 431	178, 443, 775
FCD-546-2	2529000 ± 501000	12950 ± 1378	1642000 ± 381100	4492000 ± 1031000	42, 143, 332	92, 281, 624
FCD-546-3	161900 ± 58800	920 ± 430	157200 ± 67750	233400 ± 81400	373, 663, 1210	438, 1310
FCD-660-2	2896 ± 691	423 ± 137	75690 ± 16230	29670 ± 5854	78, 219	109, 367
FCD-660-3	132200 ± 31320	4032 ± 1385	1328000 ± 303900	742800 ± 322500	41, 140, 570	120, 440, 1050
FCD-660-4	19120 ± 4151	536 ± 271	428100 ± 135200	163400 ± 63660	29, 110	71, 242, 702
LPG-IR-3	7165000 ± 980300	11410 ± 1491	7586000 ± 766400	13820000 ± 2053000	53, 138, 400	164, 436, 780
PTIR545/UF	1218000 ± 163300	1294 ± 51	488900 ± 68960	1792000 ± 227300	23, 84, 248	90, 260
PTIR550/F	258300 ± 87940	2193 ± 674	108100 ± 40190	503900 ± 191100	640, 357, 1240	522, 1490
PTIR660/F	2023 ± 287	246 ± 48	60480 ± 6536	22820 ± 2368	67, 213, 592	121, 393, 1190
		616/7 nm[e] (ND 2.0)	665/7.5 nm[e] (–)	<775 nm (ND 2.0)	616/10 nm (τ_1[d])	
Down-converting phosphor						
FL-612		n/a	208500 ± 49680	195500 ± 35510	749300 ± 126400	1030

Note. cts, counts. ND, neutral density filter. The intensities and decays were measured from 150-μl volume of 330 μg/ml phosphor suspension in DMSO at room temperature.

[a] Up-converting phosphors*:* Continuous laser excitation at 980 nm (850 nm long-pass filter) and counting for 2000 ms; Down-converting phosphor*:* pulsed Xe-flash excitation at 320 nm and time-resolved counting (400 μs delay, 400 μs counting) for 1000 cycles; intensity values are background subtracted averages of six replicates, and values are given with ± SD.

[b] Up-converting phosphors*:* Recorded using 20 μs resolution for 1000 cycles after 3.5 ms laser excitation at 980 nm; Down-converting phosphor*:* recorded using 20 μs resolution for 100 cycles after pulsed Xe-flash excitation (<10 μs) at 265 nm.

[c] Anti-stokes photoluminescence background with 535/50 nm (without ND 3.0) and 616/7 nm filters were 142 ± 38 cts and 101 ± 19 cts, respectively.

[d] The decay curves were fitted either to single, double or triple exponential decay giving one, two or three lifetimes ordered with decreasing amplitude. Uncertainty in lifetimes was typically less than 5%. Only decay times with relative amplitude over 2% are shown.

[e] Time-resolved fluorescence background with 616/7 nm (without ND 2.0) and 665/7.5 nm filters were 224 ± 69 cts and 928 ± 73 cts, respectively.

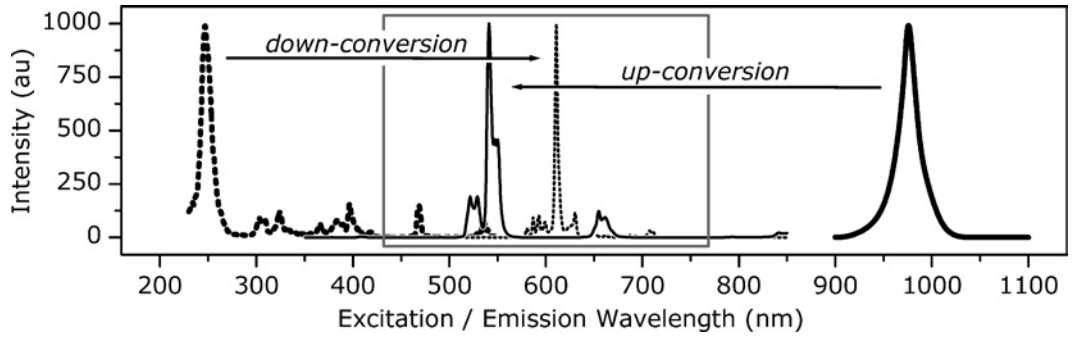

Fig. 3. Down-converted and up-converted photoluminescence of inorganic lanthanide phosphors. Photoluminescence excitation (*wide lines*) and emission (*narrow lines*) spectra of both FL-612 down-converting (*dashed lines*) and PTIR550/F up-converting (*solid lines*) phosphors. The excitation and emission spectra of FL-612 were temporally resolved from background. Excitation spectra of PTIR550/F was obtained from the manufacturer. The insert (*gray rectangle*) outlines the photoluminescence emission wavelength range 450–750 nm. *Note*. au, arbitrary unit.

components of both the green and the red emission, however, are likely to result from re-population of $^4F_{7/2}$ from $^4I_{11/2}$ by ion–ion energy transfer from $^4I_{11/2}$ level (Er^{3+}) or $^2F_{5/2}$ level (Yb^{3+}) [49]. The $^4F_{9/2}$ level can also be re-populated by the ion–ion energy transfer directly from $^4I_{13/2}$ level. The blue emission band from transition $^2H_{9/2} \rightarrow {}^4I_{15/2}$ observed at 410 nm in the spectra is a result of a three-photon process, where $^2H_{9/2}$ is excited from $^4F_{9/2}$ [47]. The weak near-infrared emission band observable at 840 nm is associated to transition $^4S_{3/2} \rightarrow {}^4I_{13/2}$.

The longest decay times were observed for the FCD-546-3 and PTIR550/F phosphors based on yttriumfluoride, which is known as an efficient host material for up-conversion [51] and has a low phonon energy resulting in longer level lifetimes of dope ions. The photoluminescence intensity of the characterized yttriumfluoride-based phosphors, however, was clearly weaker than that of the oxysulphide-based phosphors, which included also significantly shorter decay time components. The importance of the host material is supported by the observation of almost identical decay times for the two lanthanum oxysulphide-based phosphors FCD-546-1 and LPG-IR-3 obtained from different manufacturers. The small difference in the emission decay times between the two yttriumfluoride-based phosphors is most likely a consequence of slower cross-relaxation processes in PTIR550/F due to the lower Er^{3+} dope concentration. The multiple decay times of the up-converting phosphors are at least partially related to effect of the solvent; this was confirmed by observation of a single exponential decay from solid PTIR550/F phosphor both at green and red emission wavelength (data not shown). The decay of the FL-612 down-converting phosphor in DMSO was strictly single exponential (Fig. 5B) with a decay time of 1031 μs.

The commercial up-converting phosphor materials evaluated here were as such too large in average diameter to be employed as reporters in ligand binding assays. To demonstrate the possibility to process the commercial phosphors into submicron particulates suitable for reporter applications, the PTIR550/F phosphor was ground in a miniature bead mill. The average particle size of the up-converting nanoparticles in the colloidal suspension was 270 nm. The achieved particle size was

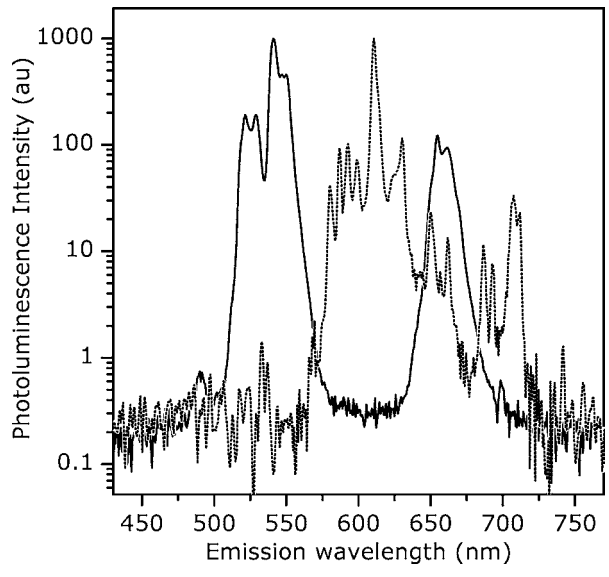

Fig. 4. Log-scale emission spectra of PTIR550/F and FL-612 phosphors. IR laser-excited anti-Stokes photoluminescence spectrum of PTIR550/F phosphor (*solid line*) and ultraviolet-excited time-resolved fluorescence spectrum of FL-612 phosphor (*dashed line*). The spectra were measured in DMSO at room temperature. The phosphor concentrations were 33 μg/ml (PTIR550/F) and 200 μg/ml (FL-612). *Note*. au, arbitrary unit.

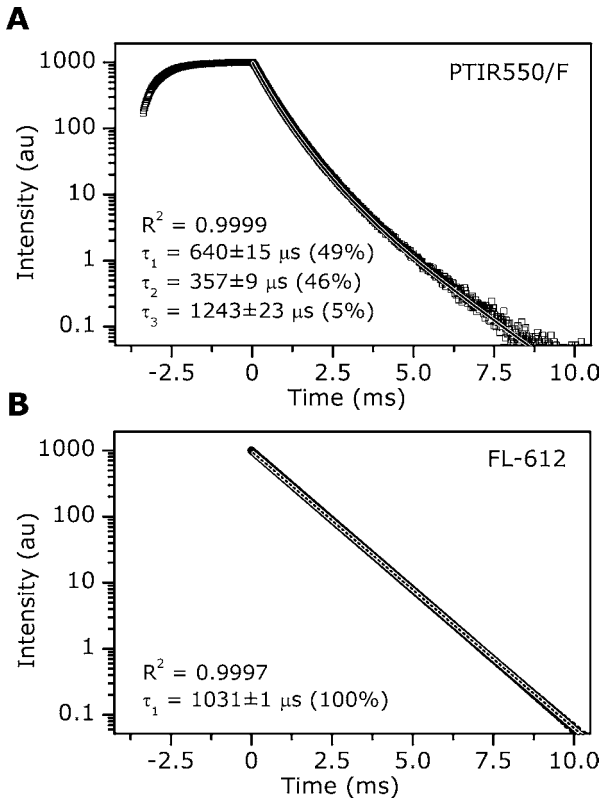

Fig. 5. Log-scale decay spectra of PTIR550/F and FL-612 phosphors. Background subtracted photoluminescence emission decay of (A) IR laser-excited PTIR550/F anti-Stokes phosphor measured at 535/50 nm (fitted to $y = A_1e^{-t/\tau_1} + A_2e^{-t/\tau_2} + A_3e^{-t/\tau_3}$) and (B) ultraviolet-excited FL-612 phosphor measured at 612/10 nm (fitted to $y = A_1e^{-t/\tau_1}$). The decay times are given with ±SD, and the percentages represent the relative amplitudes of each decay time. The decay spectra were measured from 33 μg/ml (PTIR550/F) and 200 μg/ml (FL-612) phosphor suspension in DMSO at room temperature. *Note*. au, arbitrary unit.

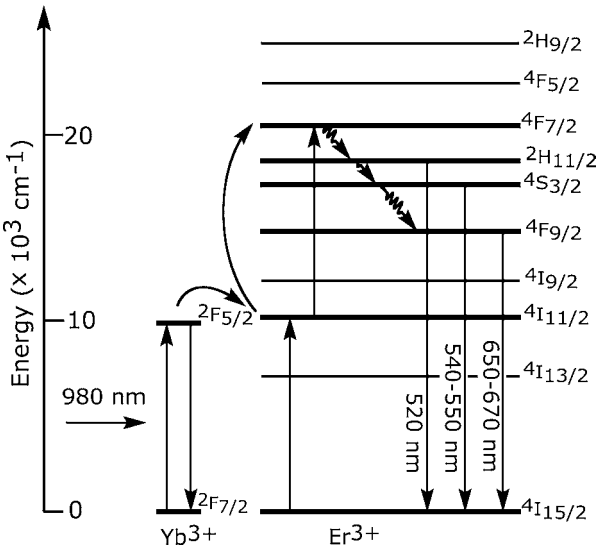

Fig. 6. Energy state diagram of the sequential energy-transfer-based up-conversion process in a Yb^{3+} and Er^{3+} doped up-converting phosphor. The absorber ion (Yb^{3+}) is excited under infrared light ${}^2F_{7/2} \rightarrow {}^2F_{5/2}$, and the energy is transferred non-radiatively from the absorber ion to the emitter ion (Er^{3+}) to first excite the ion from a ground state to a metastable state ${}^4I_{15/2} \rightarrow {}^4I_{11/2}$, and subsequently to an excited state ${}^4I_{11/2} \rightarrow {}^4F_{7/2}$. The excited state relaxes to multiple emissive states mainly through non-radiative processes, and the green and the red emission bands are assigned to radiative transitions ${}^2H_{11/2} \rightarrow {}^4I_{15/2}$, ${}^4S_{3/2} \rightarrow {}^4I_{15/2}$ and ${}^4F_{9/2} \rightarrow {}^4I_{15/2}$.

slightly smaller than reported for up-converting phosphor reporters employed in ligand binding assays [40,43,52]. The phosphor suspension appeared as transparent solution and it generated bright green light (Fig. 7) when illuminated with an infrared laser pointer at 980 nm. Recently, several reports have been published about inorganic synthesis of up-converting phosphor nanoparticles with blue, green and red emission [53–55] and the first observations of visible anti-Stokes photoluminescence from transparent nanoparticle colloids [56,57] have further promoted the development of potential applications for these particulate reporters with very attractive properties. It is obvious, that the up-converting phosphor nanoparticles equal or preferably less than 100 nm in diameter would be more appropriate for reporter applications [26,58], provided that the specific activity of the phosphor material is

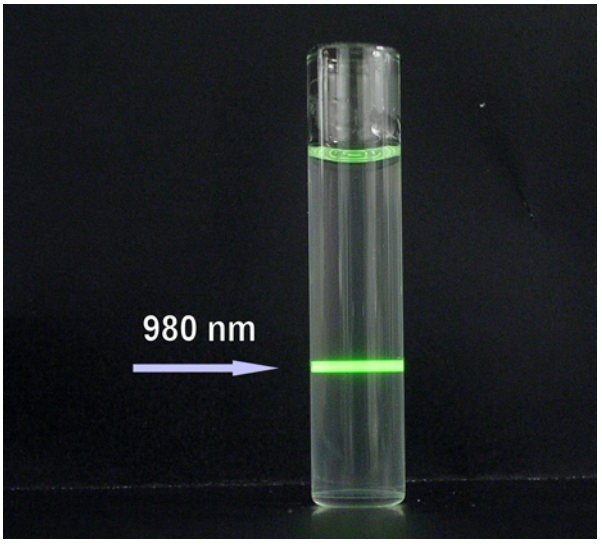

Fig. 7. Green emission of colloidal PTIR550/F up-converting phosphor preparation. A beam of an infrared laser pointer (980 nm, 100 mW, Roithner Lasertechnik) was directed to a glass vial containing colloidal PTIR550/F up-converting phosphor particles diluted to DMSO at concentration 2900 μg/ml. Picture was taken through a 775 nm short-pass filter.

retained. Unfortunately, the specific activity of the commercial TAL-IR up-converting phosphor material (an average diameter below 100 nm) was not comparable with the larger phosphors.

The characterized up-converting phosphor materials facilitate the development of new biochemical assay methods based on anti-Stokes photoluminescence and are measurable with inexpensive modifications to current instrumentation. Methods for bead-milling and bioconjugation of submicron inorganic lanthanide phosphor particles have been reported earlier [31,35,45], and these methods have been also employed for up-converting phosphors [39,40,43], but until now reports have been based on a proprietary phosphor material. Up-converting reporters have also been applied to various ligand binding assays with outstanding performance [46,52,59]. Although the particulate up-converting phosphor reporters lack one of the requirements for an ideal label, the small molecular size, the other requirements are fulfilled enabling development of sensitive ligand binding assays suitable for an inexpensive detection system–a combination of requirements, which has been very hard to meet otherwise. The potential applications of up-converting inorganic lanthanide phosphors seem even more versatile than that of the time-resolved fluorometry and ultraviolet-excited down-converting lanthanide compounds [60,61].

CONCLUSIONS

We have characterized commercially available up-converting inorganic lanthanide phosphors to evaluate the possibility to employ these materials as particulate reporters in various ligand binding assays. The unique luminescence properties of these compounds, being able to generate anti-Stokes photoluminescence with power densities significantly lower than required for two-photon excitation, are based on sequential energy transfer between trivalent rare earth ions doped in inorganic host lattice. In opposite to the down-converting lanthanide compounds, known for their characteristics luminescence properties, the up-converting phosphors provide equivalent narrow emission bands at visible wavelengths, but under infrared illumination. The total rejection of background fluorescence by an inexpensive instrumentation renders up-conversion an attractive alternative to the time-resolved fluorescence widely employed in biomedical applications.

ACKNOWLEDGMENTS

The work in this study was conducted with the support of Tekes, the National Technology Agency of Finland, and the Academy of Finland (grant no 209417). The authors thank Juhani Aalto from Hidex Oy for technological support in modification of the plate reader for anti-Stokes photoluminescence measurement, Mika Lastusaari from University of Turku for X-ray powder diffraction measurements, and Paul Ek from Åbo Akademi University for element analysis of the phosphors.

REFERENCES

1. R. P. Ekins (1987). An overview of present and future ultrasensitive non-isotopic immunoassay development. *Clin. Biochem. Revs.* **8**, 12–23.
2. R. P. Ekins (1998). Ligand assays: from electrophoresis to miniaturized microarrays. *Clin. Chem.* **44**, 2015–2030.
3. L. J. Kricka (1999). Nucleic acid detection technologies—Labels, strategies, and formats. *Clin. Chem.* **45**, 453–458.
4. E. Soini and I. Hemmilä (1979). Fluoroimmunoassay: Present status and key problems. *Clin Chem* **25**, 353–361.
5. I. Hemmilä (1985). Fluoroimmunoassays and immunofluorometric assays. *Clin. Chem.* **31**, 359–370.
6. R. P. Ekins and S. Dakubu (1985). The development of high sensitivity pulsed light, time-resolved fluoroimmunoassays. *Pure Appl. Chem.* **57**, 437–482.
7. E. D. Sevier, G. S. David, J. Martinis, W. J. Desmond, R. M. Bartholomew, and R. Wang (1981). Monoclonal antibodies in clinical immunology. *Clin. Chem.* **27**, 1797–1806.
8. G. S. David and H. E. Greene (1984) Immunometric assays using monoclonal antibodies US Patent 4,486,530.
9. R. P. Ekins (1989). A shadow over immunoassay. *Nature* **340**, 256–258.
10. R. P. Ekins (1978). Quality control and assay design. in *Radioimmunoassay and related procedures in medicine*, International Atomic Energy Agency, Vienna, pp. 39–56.
11. T. M. Jackson, N. J. Marshall, and R. P. Ekins (1983). Optimisation of immunoradiometric (labelled antibody) assays. In W. M. Hunter and J. E. T. Corrie (Eds.), *Immunoassays for Clinical Chemistry*, Churchill Livingstone, Edinburgh, pp. 557–575.
12. L. J. Kricka (1994). Selected strategies for improving sensitivity and reliability of immunoassays. *Clin. Chem.* **40**, 347–357.
13. E. Soini and H. Kojola (1983). Time-resolved fluorometer for lanthanide chelates—A new generation of nonisotopic immunoassays. *Clin. Chem.* **29**, 65–68.
14. E. Soini and T. Lövgren (1987). Time-resolved fluorescence of lanthanide probes and applications in biotechnology. *CRC Crit. Rev. Anal. Chem.* **18**, 105–154.
15. S. Dakubu and R. P. Ekins (1985). The fluorometric determination of europium ion concentration as used in time-resolved fluoroimmunoassay. *Anal. Biochem.* **144**, 20–26.
16. H. Siitari, I. Hemmilä, E. Soini, T. Lövgren, and V. Koistinen (1983). Detection of hepatitis B surface antigen using time-resolved fluoroimmunoassay. *Nature* **301**, 258–260.
17. I. Hemmilä, S. Dakubu, V.-M. Mukkala, H. Siitari, and T. Lövgren (1984). Europium as a label in time-resolved immunofluorometric assays. *Anal. Biochem.* **137**, 335–343.
18. B. Alpha, V. Balzani, J.-M. Lehn, S. Perathoner, and N. Sabbatini (1987). Luminescence probes: The Eu^{3+}- and Tb^{3+}-cryptates of polypyridine macrobicyclic ligands. *Angew. Chem. Int. Ed. Engl.* **26**, 1266–1267.
19. H. Takalo, V. M. Mukkala, H. Mikola, P. Liitti, and I. Hemmilä (1994). Synthesis of europium(III) chelates suitable for labeling of bioactive molecules. *Bioconjug. Chem.* **5**, 278–282.
20. P. von Lode, J. Rosenberg, K. Pettersson, and H. Takalo (2003). A europium chelate for quantitative point-of-care immunoassays using direct surface measurement. *Anal. Chem.* **75**, 3193–3201.

21. H. Hakala, P. Liitti, K. Puukka, J. Peuralahti, K. Loman, J. Karvinen, P. Ollikka, A. Ylikoski, V.-M. Mukkala, and J. Hovinen (2002). Novel luminescent samarium(III) chelates. *Inorg. Chem. Commun.* **5**, 1059–1062.
22. J. Karvinen, P. Hurskainen, S. Gopalakrishnan, D. Burns, U. Warrior, and I. Hemmila (2002). Homogeneous time-resolved fluorescence quenching assay (LANCE) for caspase-3. *J. Biomol. Screen.* **7**, 223–231.
23. I. Hemmilä, V. M. Mukkala, M. Latva, and P. Kiilholma (1993). Di- and tetracarboxylate derivatives of pyridines, bipyridines and terpyridines as luminogenic reagents for time-resolved fluorometric determination of terbium and dysprosium. *J. Biochem. Biophys. Methods* **26**, 283–290.
24. Y.-Y. Xu, K. Pettersson, K. Blomberg, I. Hemmilä, H. Mikola, and T. Lövgren (1992). Simultaneous quadruple-label fluorometric immunoassay of thyroid-stimulating hormone, 17-α-hydroxyprogesterone, immunoreactive trypsin, and creatine kinase MM isoenzyme in dried blood spots. *Clin. Chem.* **38**, 2038–2043.
25. E. P. Diamandis (1991). Multiple labeling and time-resolvable fluorophores. *Clin. Chem.* **37**, 1486–1491.
26. H. Härmä, T. Soukka, and T. Lövgren (2001). Europium nanoparticles and time-resolved fluorescence for ultrasensitive detection of prostate-specific antigen. *Clin. Chem.* **47**, 561–568.
27. G. Mathis (1993). Rare earth cryptates and homogeneous fluoroimmunoassays with human sera. *Clin. Chem.* **39**, 1953–1959.
28. K. Blomberg, P. Hurskainen, and I. Hemmilä (1999). Terbium and rhodamine as labels in a homogeneous time-resolved fluorometric energy transfer assay of the beta subunit of human chorionic gonadotropin in serum. *Clin. Chem.* **45**, 855–861.
29. K. Stenroos, P. Hurskainen, S. Eriksson, I. Hemmilä, K. Blomberg, and C. Lindqvist (1998). Homogeneous time-resolved IL-2-IL-2R alpha assay using fluorescence resonance energy transfer. *Cytokine* **10**, 495–499.
30. L. Kokko, K. Sandberg, T. Lövgren, and T. Soukka (2004). Europium(III) chelate-dyed nanoparticles as donors in a homogeneous proximity-based immunoassay for estradiol. *Anal. Chim. Acta.* **503**, 155–162.
31. H. B. Beverloo, A. van Schadewijk, H. J. M. A. A. Zijlmans, and H. J. Tanke (1992). Immunochemical detection of proteins and nucleic acids on filters using small luminescent inorganic crystals as markers. *Anal. Biochem.* **203**, 326–334.
32. K. Kömpe, H. Borchert, J. Storz, A. Lobo, S. Adam, T. Möller, and M. Haase (2003). Green-emitting CePO4:Tb/LaPO4 core-shell nanoparticles with 70% photoluminescence quantum yield. *Angew. Chem. Int. Ed. Engl.* **42**, 5513–5516.
33. J. W. Stouwdam, G. A. Hebbink, J. Huskens, and F. C. van Veggel (2004). Lanthanide-doped nanoparticles with excellent luminescent properties in organic media. *Chem. Mater.* **15**, 4604–4616.
34. R. Bazzi, M. A. Flores, C. Louis, K. Lebbou, W. Zhang, C. Dujardin, S. Roux, B. Mercier, G. Ledoux, E. Bernstein, P. Perriat, and O. Tillement (2004). Synthesis and properties of europium-based phosphors on the nanometer scale: Eu2O3, Gd2O3:Eu, and Y2O3:Eu. *J. Colloid Interface Sci.* **273**, 191–197.
35. H. B. Beverloo, A. van Schadewijk, S. van Gelderen-Boele, and H. J. Tanke (1990). Inorganic phosphors as new luminescent labels for immunocytochemistry and time-resolved microscopy. *Cytometry* **11**, 784–792.
36. K. Bohmann, W. Hoheisel, B. Köhler, and I. Dorn (2003) Assay basierend auf dotierten nanoteilchen Deutsches Patent- und Markenamt DE 101 53 829 A1.
37. J. Feng, G. Shan, A. Maquieira, M. E. Koivunen, B. Guo, B. D. Hammock, and I. M. Kennedy (2003). Functionalized europium oxide nanoparticles used as a fluorescent label in an immunoassay for atrazine. *Anal. Chem.* **75**, 5282–5286.
38. M. H. V. Werts, M. A. Duin, J. W. Hofstraat, and J. W. Verhoeven (1999). Bathochromicity of Michler's ketone upon coordination with lanthanide(III) beta-diketonates enable efficient sensitisation of Eu^{3+} for luminescence under visible light excitation. *Chem. Commun.* **1999**, 799–800.
39. W. H. Wright, N. A. Mufti, N. T. Tagg, R. R. Webb, and L. V. Schneider (1997). High-sensitivity immunoassay using a novel up-converting phosphor reporter. *Proc. SPIE - Int. Soc. Opt. Eng.* **2985**, 248–255.
40. H. J. M. A. A. Zijlmans, J. Bonnet, J. Burton, K. Kardos, T. Vail, R. S. Niedbala, and H. J. Tanke (1999). Detection of cell and tissue surface antigens using up-converting phosphors: A new reporter technology. *Anal. Biochem.* **267**, 30–36.
41. F. Auzel (2002). Up-conversion in rare-earth-doped systems: past, present and future. *Proc. SPIE - Int. Soc. Opt. Eng.* **4766**, 179–190.
42. J. Lakowicz (1997). *Topics in fluorescence spectroscopy, Vol. 5, Nonlinear and two-photon-induced fluorescence,* Plenum Press, New York.
43. R. S. Niedbala, H. Feindt, K. Kardos, T. Vail, J. Burton, B. Bielska, S. Li, D. Milunic, P. Bourdelle, and R. Vallejo (2001). Detection of analytes by immunoassay using up-converting phosphor technology. *Anal. Biochem.* **293**, 22–30.
44. R. T. Wegh, H. Donker, K. D. Oskam, and A. Meijerink (1999). Visible quantum cutting in LiGdF4:Eu3+ through downconversion. *Science* **283**, 663–666.
45. H. B. Beverloo, A. van Schadewijk, J. Bonnet, R. van der Geest, R. Runia, N. P. Verwoerd, J. Vrolijk, J. S. Ploem, and H. J. Tanke (1992). Preparation and microscopic visualization of multicolor luminescent immunophosphors. *Cytometry* **13**, 561–570.
46. J. Hampl, M. Hall, N. A. Mufti, Y. M. Yao, D. B. MacQueen, W. H. Wright, and D. E. Cooper (2001). Upconverting phosphor reporters in immunochromatographic assays. *Anal. Biochem.* **288**, 176–187.
47. F. Song, M. Myers, S. Jiang, Y. Feng, X. B. Chen, and G. Y. Zhang (1999). Effect of erbium concentration on upconversion luminescence of Er:Yb:phosphate glass excited by InGaAs laser diode. *Proc. SPIE - Int. Soc. Opt. Eng.* **3622**, 182–188.
48. J. Karvinen, A. Elomaa, M. L. Makinen, H. Hakala, V. M. Mukkala, J. Peuralahti, P. Hurskainen, J. Hovinen, and I. Hemmila (2004). Caspase multiplexing: Simultaneous homogeneous time-resolved quenching assay (TruPoint) for caspases 1, 3, and 6. *Anal. Biochem.* **325**, 317–325.
49. V. K. Bogdanov, D. J. Booth, and W. E. K. Gibbs (2003). Energy transfer processes and the green fluorescence in heavily doped Er3+: Fluoride glasses. *J. Non-Cryst. Solids* **321**, 1–135.
50. N. M. P. Low and A. L. Major (1971). Effects of preparation on the anti-stokes luminescence of Er-activated rare-earth phosphors. *J. Lumin.* **4**, 357–368.
51. F. Auzel (2004). Upconversion and anti-Stokes processes in f and d ions in solids. *Chem. Rev.* **104**, 139–173.
52. F. van De Rijke, H. Zijlmans, S. Li, T. Vail, A. K. Raap, R. S. Niedbala, and H. J. Tanke (2001). Up-converting phosphor reporters for nucleic acid microarrays. *Nat. Biotechnol.* **19**, 273–276.
53. G. Yi, B. Sun, F. Yang, D. Chen, Y. Zhou, and J. Cheng (2002). Synthesis and characterization of high-efficiency nanocrystal up-conversion phosphors: Ytterbium and erbium codoped lanthanum molybdate. *Chem. Mater.* **14**, 2910–2914.
54. T. Hirai and T. Orikoshi (2004). Preparation of yttrium oxysulfide phosphor nanoparticles with infrared-to-green and -blue upconversion emission using an emulsion liquid membrane system. *J. Colloid Interface Sci.* **273**, 470–477.
55. T. Hirai and T. Orikoshi (2004). Preparation of Gd2O3:Yb,Er and Gd2O2S:Yb,Er infrared-to-visible conversion phosphor ultrafine particles using an emulsion liquid membrane system. *J. Colloid Interface Sci.* **269**, 103–108.
56. S. Heer, O. Lehmann, M. Haase, and H. U. Güdel (2003). Blue, green, and red upconversion emission from lanthanide-doped LuPO4 and YbPO4 nanocrystals in a transparent colloidal solution. *Angew. Chem. Int. Ed. Engl.* **42**, 3179–3182.
57. S. Heer, K. Kömpe, H.-U. Güdel, and M. Haase (2004). Highly efficient multicolour upconversion emission in transparent colloids of nanoparticle-doped NaYF4 nanocrystals. *Adv. Mater.* **16**, 2102–2105.
58. T. Soukka, H. Härmä, J. Paukkunen, and T. Lövgren (2001). Immunoassays based on multivalent nanoparticle-antibody

bioconjugates utilize kinetically enhanced monovalent binding affinity. *Anal. Chem.* **73**, 2254–2260.
59. P. L. Corstjens, M. Zuiderwijk, M. Nilsson, H. Feindt, R. Sam Niedbala, and H. J. Tanke (2003). Lateral-flow and up-converting phosphor reporters to detect single-stranded nucleic acids in a sandwich-hybridization assay. *Anal. Biochem.* **312**, 191–200.
60. I. Hemmilä and V.-M. Mukkala (2001). Time-resolution in fluorometry technologies, labels, and applications in bioanalytical assays. *Crit. Rev. Clin. Lab. Sci.* **38**, 441–519.
61. T. Steinkamp and U. Karst (2004). Detection strategies for bioassays based on luminescent lanthanide complexes and signal amplification. *Anal. Bioanal. Chem.* **380**, 24–30.